© 2025 Journal of Pharmacy & Pharmacognosy Research, 13 (2), 606-620, 2025
ISSN 0719-4250
https://jppres.com

DOI: https://doi.org/10.56499/jppres24.2024_13.2.606

Original Article

Arctigenin and biochanin A impact on MDA-MB-231 breast cancer cells: *In silico* and *in vitro* analysis

[Efecto de la arctigenina y la biocanina A sobre las células de cáncer de mama MDA-MB-231: Análisis *in silico* e *in vitro*]

Ade Arsianti[1,3*], Miftahul Khair Akbar[2], Linda Erlina[1]

[1]Department of Medical Chemistry, Faculty of Medicine, Universitas Indonesia, Jakarta, Indonesia.
[2]Master's Programme in Biomedical Sciences, Faculty of Medicine, Universitas Indonesia, Jakarta, Indonesia.
[3]Drug Development Research Center, Faculty of Medicine, Universitas Indonesia, Jakarta, Indonesia.
*E-mail: miftahulk04@gmail.com, ade.arsianti@ui.ac.id

Abstract

Context: Breast cancer remains a leading cause of mortality among women, with triple-negative breast cancer (TNBC) being particularly aggressive. Phytoestrogens have shown potential as anti-cancer agents by reducing cancer cell viability and promoting apoptosis. This study investigates the anticancer effects of arctigenin and biochanin A, identified through molecular simulations, against TNBC.

Aims: To assess the anticancer activity of arctigenin and biochanin A, alongside tamoxifen and doxorubicin as controls, using the MDA-MB-231 cell line.

Methods: Molecular simulations were employed to identify arctigenin and biochanin A as potential compounds. The MTT assay and flow cytometry were utilized to evaluate their anticancer activity compared to tamoxifen and doxorubicin.

Results: Both the MTT assay and flow cytometry demonstrated significant anticancer activity for arctigenin and biochanin A in the MDA-MB-231 cell line.

Conclusions: The findings indicate that arctigenin and biochanin A exhibit promising anticancer properties against TNBC. Further research is essential to explore their mechanisms of action and efficacy in more complex biological systems. This study highlights the role of bioinformatics tools and experimental validation in identifying potential treatments for TNBC.

Keywords: apoptosis; bioinformatics; breast cancer; MDA-MB-231 cell line; phytoestrogen.

Resumen

Contexto: El cáncer de mama sigue siendo una de las principales causas de mortalidad entre las mujeres, siendo el cáncer de mama triple negativo (CMN) particularmente agresivo. Los fitoestrógenos han demostrado tener potencial como agentes anticancerígenos al reducir la viabilidad de las células cancerosas y promover la apoptosis. Este estudio investiga los efectos anticancerígenos de la arctigenina y la biochanina A, identificados mediante simulaciones moleculares, contra el CMN.

Objetivos: Evaluar la actividad anticancerígena de la arctigenina y la biochanina A, junto con tamoxifeno y doxorrubicina como controles, utilizando la línea celular MDA-MB-231.

Métodos: Se emplearon simulaciones moleculares para identificar la arctigenina y la biochanina A como compuestos potenciales. Se utilizaron el ensayo MTT y la citometría de flujo para evaluar su actividad anticancerígena en comparación con el tamoxifeno y la doxorrubicina.

Resultados: Tanto el ensayo MTT como la citometría de flujo demostraron una actividad anticancerígena significativa para la arctigenina y la biochanina A en la línea celular MDA-MB-231.

Conclusiones: Los hallazgos indican que la arctigenina y la biochanina A exhiben propiedades anticancerígenas prometedoras contra el cáncer de mama triple negativo. Es esencial realizar más investigaciones para explorar sus mecanismos de acción y eficacia en sistemas biológicos más complejos. Este estudio destaca el papel de las herramientas bioinformáticas y la validación experimental en la identificación de posibles tratamientos para el cáncer de mama triple negativo.

Palabras Clave: apoptosis; bioinformática; cáncer de mama; fitoestrógeno; línea celular MDA-MB-231.

ARTICLE INFO
Received: March 22, 2024.
Accepted: October 11, 2024.
Available Online: November 13, 2023.

AUTHOR INFO
ORCID: 0000-0001-5539-5642 (AA) 0000-0003-1108-0600 (LE)
0009-0006-0646-9960 (MKA)

INTRODUCTION

Breast cancer is a prevalent and significant global health issue, being the most diagnosed cancer and a leading cause of cancer-related deaths. In Indonesia, it ranks first in the number of cancer cases and contributes significantly to cancer mortality (Shaath et al., 2021; Sung et al., 2021). Immunohistochemical classification based on receptor expression identifies subtypes such as luminal A, luminal B, HER2-enriched, and basal-like breast cancer (Orrantia-Borunda et al., 2022). Triple-negative breast cancer (TNBC), a heterogeneous group characterized by the absence of hormonal receptors and HER2, represents 20% of breast cancer cases and tends to be more aggressive with a poorer prognosis (Collignon et al., 2016). TNBC subtypes include those with germline mutations in BRCA1 and BRCA2, as well as histological variations like infiltrating ductal carcinoma and metaplastic cancer (Freelander et al., 2021; Yin et al., 2020). Gene expression profiling further categorizes TNBC into six subtypes, each with potential treatment implications, although further research is needed to fully understand their clinical relevance (Makki, 2015).

In drug discovery, identifying new drugs with specific therapeutic interactions is crucial (Batool et al., 2019). Traditional methods, like high-throughput experimental screening, are time-consuming and expensive, while rational drug design, or reverse pharmacology, offers a cost-effective alternative (Moore et al., 2018). This approach involves identifying target proteins and screening small molecule libraries (Ferreira et al., 2015). Advances in structural and molecular biology, along with bioinformatics, have provided 3D structures for thousands of proteins, enabling structure-based drug design (SBDD). SBDD is efficient and specific, analyzing target protein structures to optimize drug candidates (Lionta et al., 2014; Moore et al., 2018). Computational techniques like structure-based virtual screening, molecular docking, and molecular dynamics simulations are commonly used in SBDD to analyze binding energetics and interactions. Automation and access to powerful computing resources have further accelerated the drug discovery process (Batool et al., 2019; Pedretti et al., 2019).

Phytoestrogens, natural compounds similar to estrogen found in plants, offer various health benefits, including preventing menopausal symptoms, type 2 diabetes, cardiovascular disease, obesity, and cancer. They possess anti-inflammatory, antitumor, antioxidant, and other properties (Torrens-Mas and Roca, 2020). Soy products containing phytoestrogens are associated with a reduced risk of breast, ovarian, and prostate cancers (Anandhi Senthilkumar et al., 2018). Phytoestrogens have been studied for their potential as anti-cancer treatments and adjuncts to conventional therapies. They offer pharmacological benefits and can inhibit the proliferation of breast cancer cells and tumor formation (Ko et al., 2018). In silico approaches, such as structural modeling and molecular docking, are used to identify potential compounds, which are then confirmed through *in vitro* tests (Mabonga and Kappo, 2019).

TNBC is a highly aggressive form of breast cancer lacking the three common receptors, estrogen, progesterone, and HER2, limiting treatment options and making the search for effective therapies critical. Phytoestrogens, plant-derived compounds that mimic estrogen, have emerged as potential candidates for TNBC treatment due to their ability to interact with estrogen receptors and influence cancer-related signaling pathways. These compounds can exert estrogenic or anti-estrogenic effects, influencing processes like cell proliferation, apoptosis, and epithelial-mesenchymal transition (EMT) (van Barele et al., 2021). For example, genistein and daidzein have shown promise in inducing apoptosis and inhibiting cell proliferation, while coumestrol has demonstrated cytotoxic effects by inhibiting non-genomic estrogen signaling, which promotes cell invasion (Torrens-Mas and Roca, 2020). Despite the potential of phytoestrogens, challenges such as poor bioavailability, lack of clinical evidence, drug resistance, variability in phytochemical composition, and complex mechanisms of action hinder their effectiveness as standalone therapies. To enhance efficacy, there is growing interest in combining phytoestrogens with conventional treatments. However, addressing these challenges, including improving bioavailability and understanding drug resistance mechanisms, is essential to fully realize the therapeutic potential of phytochemicals in TNBC treatment (Alaouna et al., 2023; Xiong et al., 2024). This study aimed to employ virtual screening and molecular simulations using a bioinformatics approach to identify the best phytoestrogen compounds for TNBC treatment, with confirmation through the MTT and flow cytometry test to evaluate cell cytotoxicity and determine candidate compound effectiveness to induce apoptosis.

MATERIAL AND METHODS

Materials

The utilized tools include a Lenovo Ideapad Slim 3 Laptop equipped with an AMD-Ryzen processor, 8 GB RAM, and a Windows 10 64-bit operating system (Lenovo, Lenovo Group Limited, China). Additional-

ly, software such as Cytoscape 3.10.1, LigandScout 4.4.8, and various databases including String, Gene Expression Omnibus (Cytoscape, Institute for Systems Biology, United States), GeneCards, LifeMap Sciences, Inc., United States, KEGG Kyoto Encyclopedia of Genes and Genomes, Kyoto University Bioinformatics Center, Japan, PubChem, National Institutes of Health (NIH), United States, EnrichR, Ma'ayan Laboratory, United States, ADMETlab, Central South University, China, pkCSM, University of Queensland, Australia, and SwissADME, SIB Swiss Institute of Bioinformatics, Switzerland were employed. Experimental equipment such as Autodock 4.2.6 from The Scripps Research Institute, United State, MarvinSKetch, ChemAxon, Hungary, Biovia Discovery Studio, Dassault Systèmes, France, Biosafety Level II Cabinet (Biobasem Biobase Bioindustry, Shandong Co., Ltd., China), CO_2 incubator from Thermo Fisher Scientific Inc, United States, inverted microscope BLD, from Suzhou Jingtong Instrument Co., Ltd., China, refrigerated centrifuge 800D, from Jiangsu Jinyi Instrument Technology Company Limited, China, micropipettes (Brand, Brandtech Scientific, Inc., Germany), hemocytometer Blaudbrand from brand GmbH, Germany, ELISA reader Diatek from Wuxi Hiwell Diatek Instruments Co., Ltd., China, as well as consumables including 96-well plates OneMed, OneMed-Medicom, Indonesia, T-25 flasks Corning from Corning Incorporated, United States, and conical tubes, microtubes, and pipette tips, were also utilized.

As for consumables, we used MDA-MB-231 cell line from the Department of Chemistry Faculty of Medicine Universitas Indonesia, fetal bovine serum Gibco, DMEM medium Gibco, 0.25% trypsin EDTA, MTT reagent, trypan blue from Gibco, and annexin V-FITC/PI apoptosis kit from Thermo Fisher Scientific, United States, dimethyl sulfoxide from Sigma Aldrich, Merck, and kGaA, arctigenin, biochanin A, tamoxifen, and doxorubicin from TCI, Japan.

Collection of genes involved in the pathway of triple-negative breast cancer

Gene data related to triple-negative breast cancer were downloaded from the GeneCards database, accessible at https://www.genecards.org/, and from the KEGG database, accessible at https://www.genome.jp/kegg/, using the keyword "triple negative breast cancer". In the pathway maps section, "human disease" was selected, followed by choosing the specification "breast cancer." Subsequently, gene data were obtained from the pathway entry section. Additionally, gene data were retrieved from the Gene Expression Omnibus (GEO) database, and Differentially Expressed Gene (DEG) analysis was conducted using the GEO2R feature on the GEO database (Barrett et al., 2019). The dataset with ID GSE185645 was selected because it was derived from patients diagnosed with triple-negative breast cancer and healthy individuals. Genes with a Log2 fold change value between -2 to 0 and 0 to 2 were selected for protein-protein interaction analysis. All gene data were collected by copying the entire list of gene names into an Excel format. The data obtained from the three databases were then used to create a Venn diagram at http://www.interactivenn.net/ to identify overlapping genes, which were subsequently compiled into an Excel file.

Protein-protein interaction

The previously obtained genes were analyzed for protein-protein interactions using the STRING web server integrated into the Cytoscape application. Protein interactions were selected based on those connected within a network with a Stringdb score of 0.999 and an experimental Stringdb score >0.9. Proteins outside the network were eliminated to ensure that only proteins with high-confidence interactions were chosen. Visualization was directly generated in Cytoscape. The visualized results were saved as PNG files, while the interaction data were saved as TSV files. Clustering of the interaction results was then conducted using the STRING web server, accessible at https://string-db.org/.

Analysis of KEGG pathway enrichment and Functional Gene Ontology (GO)

Target proteins from the protein-protein interaction analysis were then analyzed based on their functions (Park et al., 2023). The analysis involved uploading all target protein lists to the Enrichr database, accessible at https://maayanlab.cloud/Enrichr/. The analysis was conducted through KEGG pathway enrichment and Gene Ontology (GO) functional analysis, consisting of biological processes, molecular functions, and cellular components. Proteins interacting with phytoestrogen compounds were further analyzed by predicting therapeutic pathways using the ShinyGO 0.77 web server, accessible at http://bioinformatics.sdstate.edu/go/.

Virtual screening

The target proteins obtained were then searched for in the Protein Data Bank (www.rcsb.org), downloaded in PDB format, and a pharmacophore model was created based on the structure using LigandScout version 4.4.9. Virtual screening was then performed using a phytoestrogen compound database containing 1,908 compounds by collecting data on phytoestrogen compounds found in the PubChem database

(https://pubchem.ncbi.nlm.nih.gov/). The hit compounds were subjected to absorption, distribution, metabolism, and elimination (ADME) property prediction and prepared for molecular docking.

Prediction of ADME properties and toxicity

Phytoestrogen derivative compounds resulting from virtual screening were uploaded to the SwissADME, ADMETLab 2.0, and pkCSM pharmacokinetics web servers. The compounds were uploaded by obtaining the simplified molecular input line entry system (SMILES) format from PubChem. The ADME and toxicity profiles were then compiled into Microsoft Excel for further processing and data arrangement.

Molecular docking preparation

Protein preparation was carried out using the AutoDock 4.2.6 software. Proteins were separated from the native ligand and water molecules and then saved in .pdb format. Cleaned proteins were polarized with hydrogen, non-polar hydrogen atoms were removed, and Gasteiger charges were added. Binding pockets were determined using grid maps with sizes of 40 × 40 × 40, 50 × 50 × 50, and 60 × 60 × 60, based on the redocking of native ligands for docking validation on proteins with native ligands. If a protein lacked a native ligand, binding site prediction was performed first. This binding site was used as a reference point to create binding pockets in three sizes, determining the size and area of the protein's binding site. Phytoestrogen compounds resulting from screening were downloaded from PubChem in .sdf format. Compound preparation was done using the MarvinSketch software, converting them to.pdb format. The test compounds, such as the screening test compounds, tamoxifen, and doxorubicin as reference drugs, were then prepared using AutoDock 4.2.6 by converting them into files in pdbqt format.

Molecular docking and visualization

Molecular docking was conducted once protein and ligand preparation was completed. The files in PDBQT format were uploaded to AutoDock 4.2.6 software. Molecular docking was performed using the appropriate binding pocket and the Lamarckian genetic algorithm (Chen et al., 2023). The resulting output data were in dynamic process format (DPF) and ran using a command prompt. The molecular docking results were used to create a binding complex using AutoDock 4.3.6 and saved in protein data bank (PDB) format. The 2D and 3D visualizations of the molecular docking results were generated using BioVIA Discovery Studio Visualizer by importing the complex in PDB format and saving it as PNG.

Cell culture

MDA-MB-231 cell culture was initiated by taking cells from frozen stock and thawing them in a 37°C water bath for less than one minute. The thawed cells were then added to 1 mL of complete medium (DMEM, 10% FBS, and 1% P/S) and homogenized. The homogenate was transferred to a 15 mL canonical tube, and the complete medium was added until the volume reached 3 mL. The homogenate was centrifuged at 1,500 rpm for 5 minutes. The homogenate was separated into supernatant and pellet, with the supernatant discarded. In the same canonical tube, 1 mL of complete medium was added and homogenized to mix the pellet. 10 µL of homogenate was taken for counting by adding 10 µL of trypan blue and placing it in a hemocytometer counting chamber (Fadilah et al., 2024).

Viable cells were transferred to a T25 flask and given 5 mL of complete medium. The cells were pipetted using a 1,000 µL tip and spread evenly across the surface of the T25 flask. The flask containing the cells was observed under a microscope to check cell distribution before being placed in a 5% CO_2 incubator at 37°C. MDA-MB-231 cells divide at a rate of once every 24 hours and typically reach confluence in 3-4 days. The growth medium for the MDA-MB-231 culture was changed every two days, with daily monitoring of the medium.

Cytotoxic activity testing using MTT assay method

Approximately 10,000 counted cells were seeded in each well of a 96-well microplate and incubated in a 5% CO_2 incubator at 37°C for 24 hours. The cells adhered to the bottom of the well plate, and test compounds, such as the screening test compounds, tamoxifen, and doxorubicin as positive control, were added in different concentration variations, optimized from a range of 100 ppm to 1.125 ppm with 0.5 concentration intervals. The compounds were added after 24 hours of cell growth and incubated for another 24 and 48 hours (Fadilah et al., 2024).

The cells were observed under a microscope at 24 and 48 hours. The sample compounds were discarded, and 100 µL of MTT reagent at a concentration of 5 mg/mL, diluted tenfold, was added to each well. The cells were incubated for 3-4 hours. Cells treated with MTT formed purple formazan crystals, indicating live cells. The formazan crystals were dissolved using DMSO reagent after decanting the MTT reagent. Absorbance was measured using an ELISA reader at a wavelength of 630 nm. The absorbance data were used to create a concentration vs. % cytotoxicity curve in Microsoft Excel, from which the inhibition concen-

tration 50 (IC_{50}) value was determined (Fadilah et al., 2024).

Flow cytometry test

The IC_{50} value was used to establish the concentration of compounds for apoptosis activity testing using flow cytometry. Cells were analyzed for apoptosis using the annexin V-FITC/PI analysis method with the annexin V-FITC Apoptosis Detection Kit from SIGMA. 100,000 cells were seeded and incubated for 24 hours in a 5% CO_2 incubator and treated with arctigenin, biochanin A, tamoxifen, and doxorubicin at IC_{50} concentrations for 24 hours. The treated cells were harvested and washed with cold PBS. The washed cells were homogenized using a binding buffer with a total volume of 500 µL. The cells in the binding buffer were divided into two tubes, each containing 250 µL of cells. One tube served as the unstained control, while 5 µL of annexin V-FITC and 5 µL of propidium iodide (PI) were added to the second tube. The mixture (annexin and PI) was incubated for 15 minutes in the dark and quantified using the BD FACS Aria III flow cytometer (Telford, 2018). The test sample used was a duplicate.

The data obtained, such as forward scatter (FSC), side scatter (SSC), and fluorescence intensity, were collected. During pre-processing, compensation was applied to address spectral overlap between fluorophores, and quality control was performed to remove low-quality data points, such as debris and doublets. In the gating strategy, FSC and SSC were used to create a dot plot that distinguished live cells from debris, followed by quadrant analysis to divide the plot into four quadrants using two parameters on the axes, with Quadrant I (Q1) representing double positive for both markers, Quadrant II (Q2) positive for marker 1 only, Quadrant III (Q3) double negative, and Quadrant IV (Q4) positive for marker 2 only. Visualization of these gated populations was done using software that generated a four-segment diagram, with each quadrant representing a different cell population. Finally, the percentage of cells in each quadrant was analyzed to interpret the distribution and expression levels of specific markers, aiding in the identification of desired subpopulations (Telford, 2018).

Statistical analysis

KEGG pathway enrichment analysis and functional enrichment analysis using the Enrichr database. The Enrichr database revealed the top ten enriched pathways associated with breast cancer for KEGG pathway enrichment analysis. The p-values, representing the level of enrichment, were calculated using the Fisher method. The p-values were sorted in ascending order, with a smaller p-value indicating a more significant enrichment. Three factors were considered for the functional enrichment analysis of gene ontology proteins associated with breast cancer: biological processes, molecular functions, and cellular components. The enrichment results were assessed using the Fisher method. The p-values were sorted in ascending order, with a smaller p-value indicating a more significant enrichment. Analysis of protein-protein interactions was performed using STRING in Cytoscape at a confidence level of 0.9.

In silico data analysis

The data analysis for molecular docking was divided into two sections. One is for validation, and the other is for the real docking. For validation, we would pay attention to the RMSD parameter that needs to be below 2.0 A. For the real docking, we would see the binding energy and inhibition constants parameter. For binding energy, the preferable value was between -4.00 and -10.00 kcal/mol, while the inhibition constants were around nM until µM.

The data analysis for ADME and toxicity prediction was followed by Lipinski's Rule of 5 to determine the druglikeness. The Lipinski rule of 5 was allowed if the molecular weight was less than 500, HBA was less than 10, and HBD was less than 5. For pharmacokinetics, we were concerned about GI absorption and blood-brain barrier penetration. Hence, we also pay more attention to inhibiting the CYP enzyme.

RESULTS

Search through GEO database, GeneCards, and KEGG

The dataset GSE185645, which included data from 15 triple-negative breast cancer patients and 1 normal individual, was selected for the analysis of Differentially Expressed Genes (DEG) after a search using the keyword "triple negative breast cancer" in the GEO database. Through DEG analysis using GEO2R, 18,985 genes with differential expression were found, consisting of 8,160 upregulated genes and 10,715 downregulated genes, with Log2FC values between -2 and 0, and between 0 and 2. Visualization of the analysis results was done using a Volcano plot, as shown in Fig. 1.

By using the keywords "triple negative breast cancer" and "apoptosis" in the GeneCards database, 2,624 protein-coding genes were found for triple-negative breast cancer, and 12,975 protein-coding genes were found for apoptosis. In the KEGG database, 106 proteins related to breast cancer were identified. Through intersection analysis using a Venn diagram, 52 proteins were identified that appeared in all four da-

tasets, namely the DEG analysis results, triple-negative breast cancer data from GeneCards, apoptosis data from GeneCards, and breast cancer data from KEGG, as shown in Fig. 2.

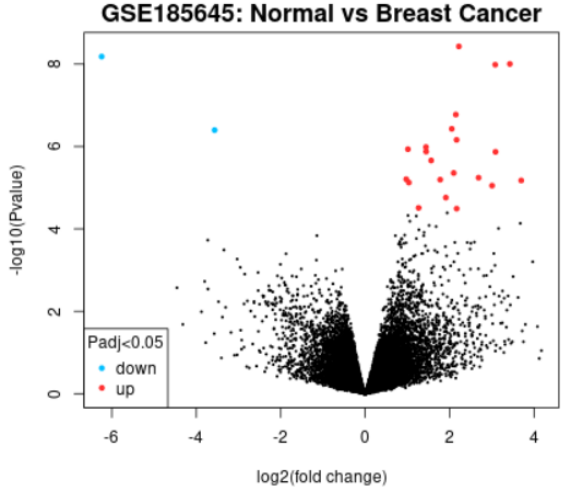

Figure 1. The Volcano Plot depicts Differentially Expressed Genes (DEGs) between normal and breast cancer samples in the GSE185645 dataset.

Genes with significantly increased expression are marked with red dots, genes with no significant change are represented by black dots, and genes with significantly decreased expression are indicated by blue dots.

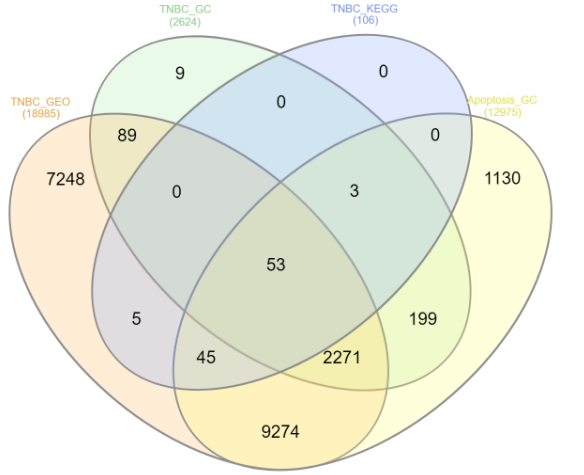

Figure 2. Venn Diagram of Common Differentially Expressed Genes (DEGs) from the GSE185645 dataset and 3 other datasets.

Formation of protein-protein interaction (PPI) network

The protein data obtained from the previous analysis was further processed to construct a protein-protein interaction (PPI) network. Out of the 52 analyzed proteins, 36 proteins with a Stringdb score of 0.999 were identified, as shown in Fig. 3.

Enrichment analysis

From the pathway analysis based on KEGG 2021 human, the proteins obtained from the PPI results were related to breast cancer. In addition to pathway analysis based on KEGG 2021 human, enrichment analysis also included GO analysis. GO consists of three components: biological processes, molecular functions, and cellular components, as shown in Table 1.

The results of the biological process analysis indicated that the proteins obtained from the PPI analysis were associated with the canonical Wnt signaling pathway as well as other Wnt signaling pathways. The molecular function analysis results showed that the proteins obtained from the PPI analysis were associated with frizzled binding function and were involved in Wnt receptor activity. The cellular component analysis results indicated that the proteins obtained from the PPI analysis were associated with endocytic vesicle membrane function and were involved in endocytic vesicle components.

Referring to the results of the protein-protein interaction and enrichment analysis, six proteins were identified as potential protein targets, namely WNT, Frizzled, LRP5/6, Dvl, GSK-30, and β-catenin, as shown in Fig. 4. The hub gene construction resulted in 10 proteins with the best interactions. The hub gene construction results showed that β-catenin had strong interactions, and in this study, β-catenin was chosen as the target because it plays a significant role in the Wnt signaling pathway, as shown in Fig. 5.

Structure-based pharmacophore model development

Structure-based pharmacophore modeling was carried out based on ligand interactions with the binding site on the CTNNB1 structure, as shown in Fig. 6. This model revealed two hydrophobic interactions involving Met243 and Val208 and one hydrogen bond acceptor, namely Ser246. These features were associated with active site residues.

Virtual screening and ADME and toxicities prediction analysis

Compounds were selected based on the ranking of pharmacophore fit scores, as shown in Table 2. This study evaluated the absorption, distribution, metabolism, excretion, and toxicity (ADMET) characteristics of the compounds arctigenin and biochanin A, using predictions made through web servers and software such as ADMETlab, SwissADME, and pkCSM.

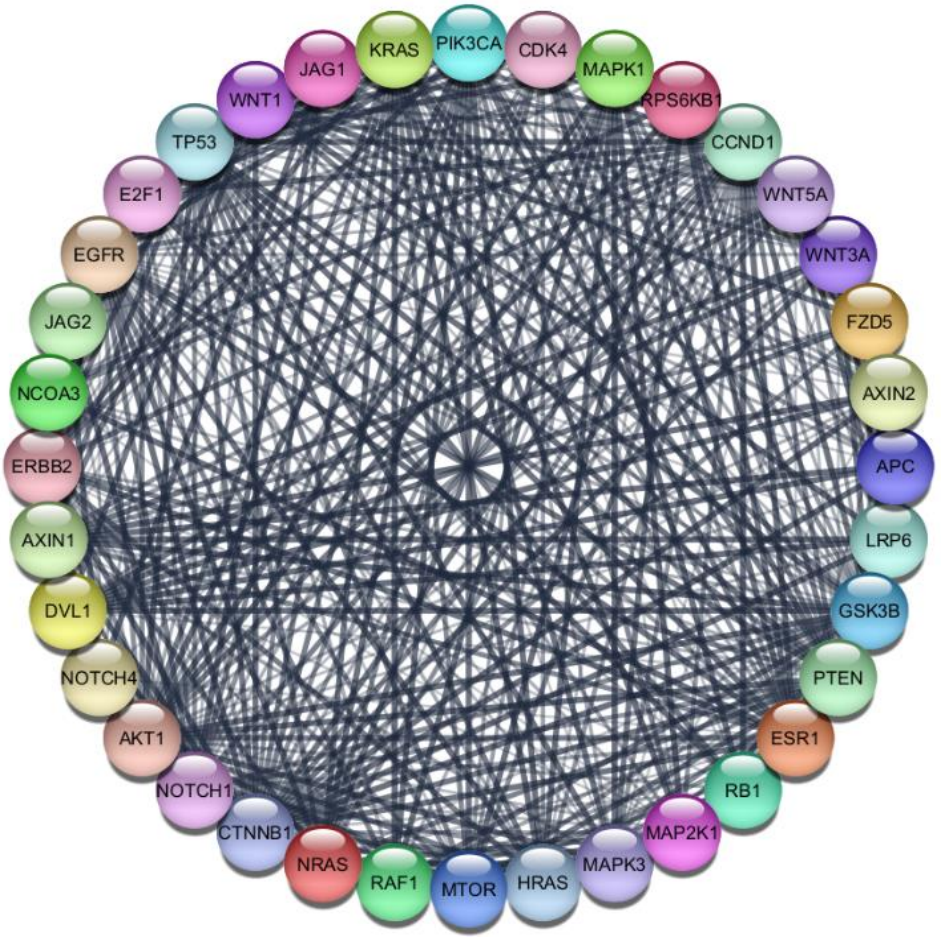

Figure 3. Protein-Protein Interaction (PPI) Network of Differentially Expressed Genes (DEGs) in the GSE185645 dataset.

Table 1. Pathways related to the 36 proteins.

Analysis	Name	P-value
Pathway	Breast cancer	1.45E-76
Gene ontology	Canonical Wnt signalling pathways	2.00E-12
	Frizzled binding	1.116E-12
	Endocytic vesicle membranes	4.698E-7

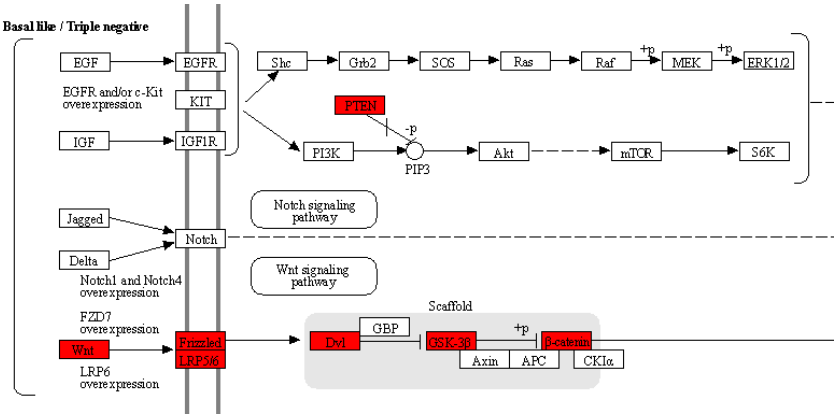

Figure 4. Prediction of protein-protein targets on the Wnt signaling pathway. Red-colored boxes represent protein targets on the Wnt signaling pathway.

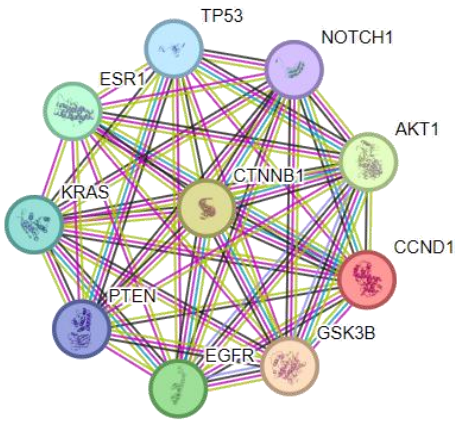

Figure 5. Hub genes formed from 10 proteins with the best-combined values.

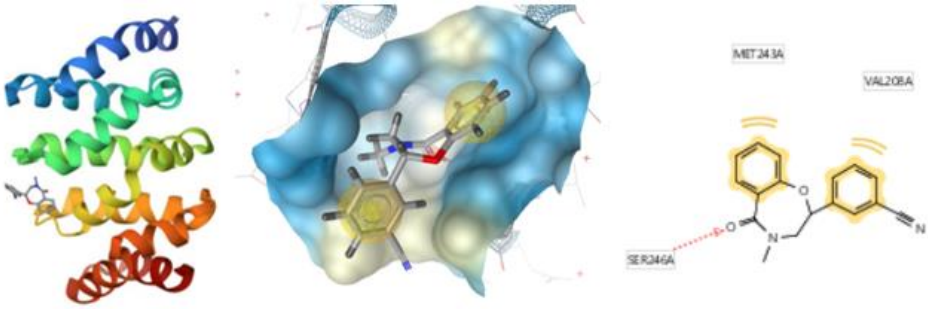

Figure 6. The pharmacophore model generated.
Protein-ligand interactions at the CTNNB1 binding site are determined to construct the pharmacophore model.

Table 2. Results obtained from pharmacophore-based screening.

No.	Compound	Pharmacophore
		Fit-Score
1	**Arctigenin**	**38.47**
2	**Biochanin A**	**38.44**
3	Daidzein	38.16
4	Genistein	38.08
5	Genistin	38.01
6	Ononin	37.83
7	Tectoridin	37.59

Both compounds met drug-likeness criteria based on Lipinski's rule of five, indicating good solubility in water, and had optimal topological polar surface area (TPSA) values. Additionally, the nRotB parameter (number of rotatable bonds) indicated good molecular flexibility.

Predictions of absorption in the human intestine indicated high absorption for both compounds. Analysis of interactions with cytochrome P450 (CYP) proteins showed that arctigenin acted as an inhibitor of CYP2C9 and CYP3A4, while biochanin A did not inhibit these enzymes. The excretion profiles of both arctigenin and biochanin A fell into the medium-clearance category, and the toxicity predictions indicated no alerts and non-hepatotoxicity, suggesting they are safe for use. Furthermore, the predicted Log D values at pH 7.4 indicated that both compounds have favorable distribution coefficients as drug candidates, as shown in Table 3.

Molecular docking

Three residues (Met243, Val208, and Ser246) were involved in the active site of the protein based on the

published crystal structure (PDB ID: 7AFW) with a resolution of 1.81 Å. The results showed that CTNNB1 had a binding site within a 50 × 50 × 50 box and XYZ coordinates of 59.556, -40.342, and 17.8, with a root-mean-square deviation (RMSD) of 0.19. Binding energy (ΔG) and Ki values from the molecular docking analysis are presented in Table 4.

The interaction of the test compounds involved hydrogen bonding and van der Waals interactions, with information on the interaction of amino acid residues in the protein depicted. The number of hydrogen and van der Waals bonds was compared with the interactions of the native ligand. The interaction studies of arctigenin and biochanin A with the protein target showed that the types of interactions formed were mostly similar to those of the native ligand. Therefore, it was concluded that arctigenin and biochanin A bind to the protein target with coordinates similar to the native ligand and are expected to have similar activity to the ligand, as shown in Table 5. The results of molecular docking are visualized in Fig. 7.

In vitro cytotoxic activity test using MTT method

Biochanin A and arctigenin, identified as promising compound candidates through *in silico* results, were tested for their toxicity on MDA-MB-231 (triple-negative breast cancer) cells using the MTT method. These compounds were tested as experimental compounds, while tamoxifen and doxorubicin were used as positive controls. The IC_{50} value, which represents the concentration at which 50% cytotoxicity occurs, was determined by creating a curve that relates the log concentration to the percentage of cytotoxicity at various concentrations. This IC_{50} value is expressed in µM after conversion from µg/mL by multiplying the molecular weight of each compound. The toxicity evaluation was performed at the 50% inhibition point, as shown in Table 6.

Table 3. Drug likeness parameter study of the two best compounds, as provided by computational prediction method.

Ligand	Parameter	Arctigenin	Biochanin A
Drug likeness	Log P	2.941	3.081
	MW	372.16	284.07
	HBA	6	5
	HBD	1	2
	NROTB	7	2
	TPSA	74.22	79.90
	Log S (log mole/L)	1.97e-02	3.42e-02
	Lipinski	Yes	Yes
Adsorption	HIA	High	High
	Caco-2 permeability (cm/s)	-4.753	-4.739
	MDCK permeability (cm/s)	2.2e-05	1.1e-05
	Pgp inhibitor	No	No
	Pgp substrate	Yes	Yes
Distribution	BBB penetration	No	No
	Fraction unbound (%)	4.763	2.457
	Log D (log mole/L)	3.325	2.772
Metabolism	Inhibitor CYP2C19	No	No
	Inhibitor CYP2C9	Yes	No
	Inhibitor CYP2D6	No	No
	Inhibitor CYP3A4	Yes	No
Excretion	Clearance (mL/min/kg)	13.272	5.872
Toxicity		No	No
	Hepatotoxicity alert	0	0

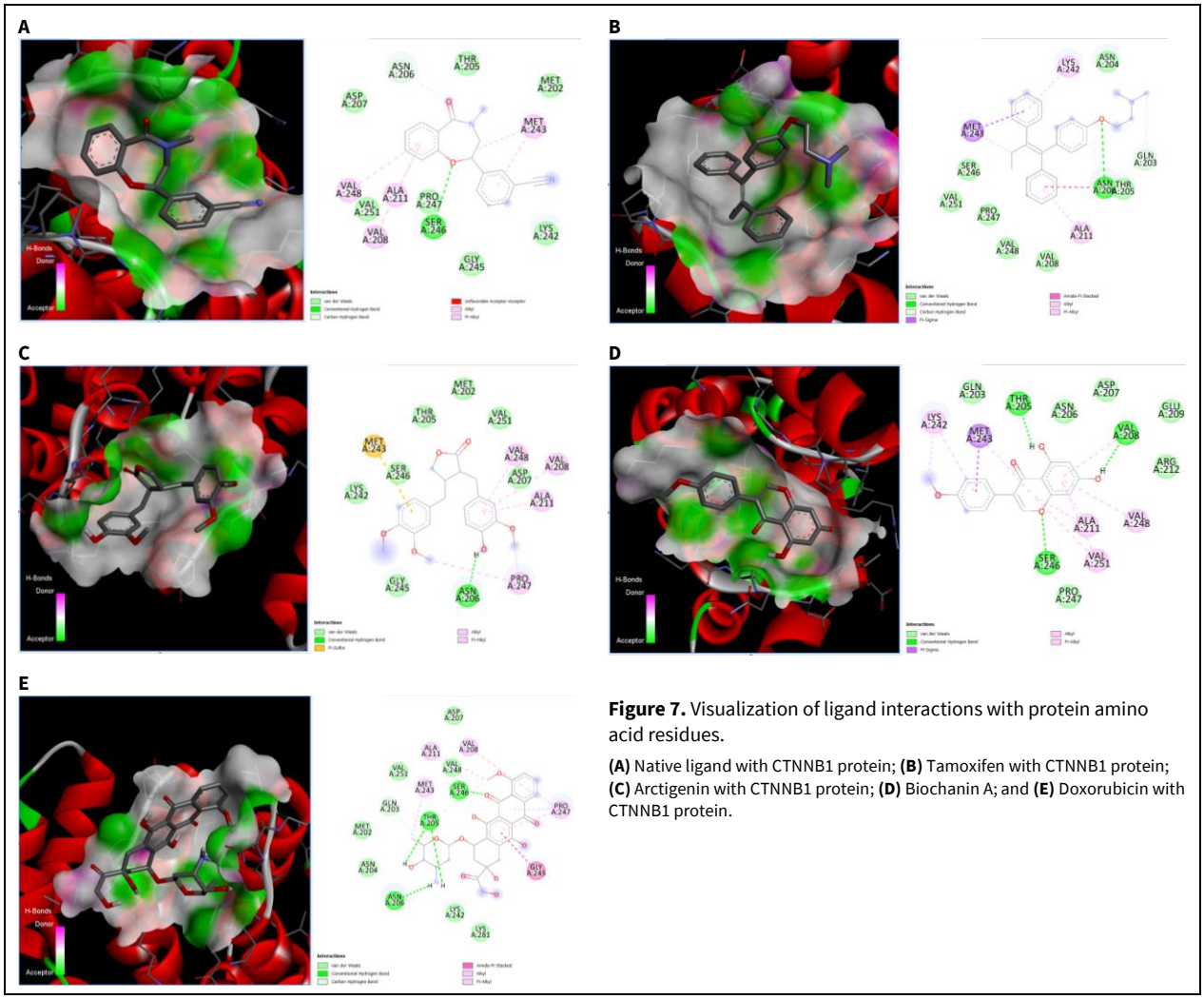

Figure 7. Visualization of ligand interactions with protein amino acid residues.

(A) Native ligand with CTNNB1 protein; **(B)** Tamoxifen with CTNNB1 protein; **(C)** Arctigenin with CTNNB1 protein; **(D)** Biochanin A; and **(E)** Doxorubicin with CTNNB1 protein.

Table 4. Results obtained from molecular docking to CTNNB1.

No	Compound	Binding energy	Constant inhibition
1	**Native ligand**	**-6.69**	**-**
2	**Arctigenin**	**-5.84**	**73.68 µM**
3	**Biochanin A**	**-5.85**	**65.51 µM**
4	Daidzein	-5.48	100.35 µM
5	Genistein	-5.63	193.65 µM
6	Genistin	-5.32	150.40 µM
7	Ononin	-5.76	109.67 µM
8	Tectoridin	-5.49	5.28 mM
9	**Tamoxifen**	**-5.50**	**92.64 µM**
10	**Doxorubicin**	**-5.09**	**187.15 µM**

Table 5. Interactions of the two best-performing compounds within the active site of CTNNB1.

No.	Compound	Amino acids of receptor 7AFW that form hydrogen bonds with the ligand	van der Waals
1	Native ligand	**Ser246**	**Thr205, Met202, Lys242, Gly245, Pro247, Val251, Asp207**
2	Tamoxifen	Asn206	Asn204, **Thr205**, Val208, Val248, **Pro247**, **Val251**, **Ser246**
3	Arctigenin	Asn206	**Gly245, Lys242, Ser246, Thr205, Met202, Val251, Asp207**
4	Biochanin A	**Ser246**, **Thr205**, Val208	**Pro247,** Gln203, Asn206, **Asp207**, Glu209, Arg212
5	Doxorubicin	**Ser246**, **Thr205**, Asn206	Lys281, **Lys242**, Asn204, **Met202**, **Val251**, Val248, **Asp207**

Table 6. IC_{50} values of cytotoxicity for arctigenin and biochanin A compounds.

No.	Compound	IC_{50} (µg/mL)	IC_{50} (µM)
1	Tamoxifen	22.40248	60.346
2	Arctigenin	15.96776	42.903
3	Biochanin A	59.64639	244.386
4	Doxorubicin	16.8605	31.040

Table 7. Percentage of MDA-MB-231 cells undergoing apoptosis.

Test sample	Total apoptosis (%)	Early Apoptosis (%)	Late apoptosis (%)	Necrosis (%)
Cell control MDA-MB-231	20.00	16.51	3.49	0.56
Tamoxifen	74.58	58.09	16.49	0
Arctigenin	91.73	35.50	56.23	0.1
Biochanin A	96.3	63.78	32.52	0
Doxorubicin	64.45	47.37	17.08	0.11

Apoptosis test on MDA-MB-231 cells using flow cytometry

After determining the concentration inhibiting the proliferation of MDA-MB-231 cells by 50%, an apoptosis activity test was conducted using double staining with annexin V/FITC and PI. The results showed that MDA-MB-231 cells treated with biochanin A and arctigenin showed the highest proportion of cells in the late apoptosis stage compared to the control MDA-MB-231 cells, as shown in Table 7. The results of flow cytometry are visualized in Fig. 8.

DISCUSSION

This study conducted KEGG pathway enrichment analysis to explore biological pathways involving protein target genes, particularly those related to breast cancer. KEGG pathways with a $p<0.05$ were identified, primarily focusing on the canonical Wnt signaling pathway, which is significant in regulating breast cancer cell proliferation. At the level of molecular function in gene ontology, there was significant identification of Frizzled binding, which is associated with the Wnt signaling pathway and has implications for triple-negative breast cancer (TNBC) (Yang et al., 2011). The analysis also revealed enrichment in the activity of the endocytic vesicle membrane, which plays a crucial role in regulating the canonical Wnt signaling pathway and endocytosis processes. These findings provide comprehensive insights into the complex relationship between the canonical Wnt signaling pathway, Frizzled binding, and endocytic vesicle membrane in the context of TNBC, laying the groundwork for understanding the molecular basis of the disease and its potential as a therapeutic target. Additionally, the study indicates that in TNBC, the canonical Wnt signaling pathway, Frizzled binding, and the endocytic vesicle membrane are interconnected, with emphasis on their roles in TNBC development.

In this study, the gene ontology in the molecular function category that was significantly enriched is the canonical Wnt signaling pathway. The canonical Wnt signaling pathway plays a critical role in breast cancer and is involved in various biological processes. This pathway is primarily responsible for the proliferation of breast cancer cells. Dysregulation of the canonical Wnt signaling pathway has been linked to

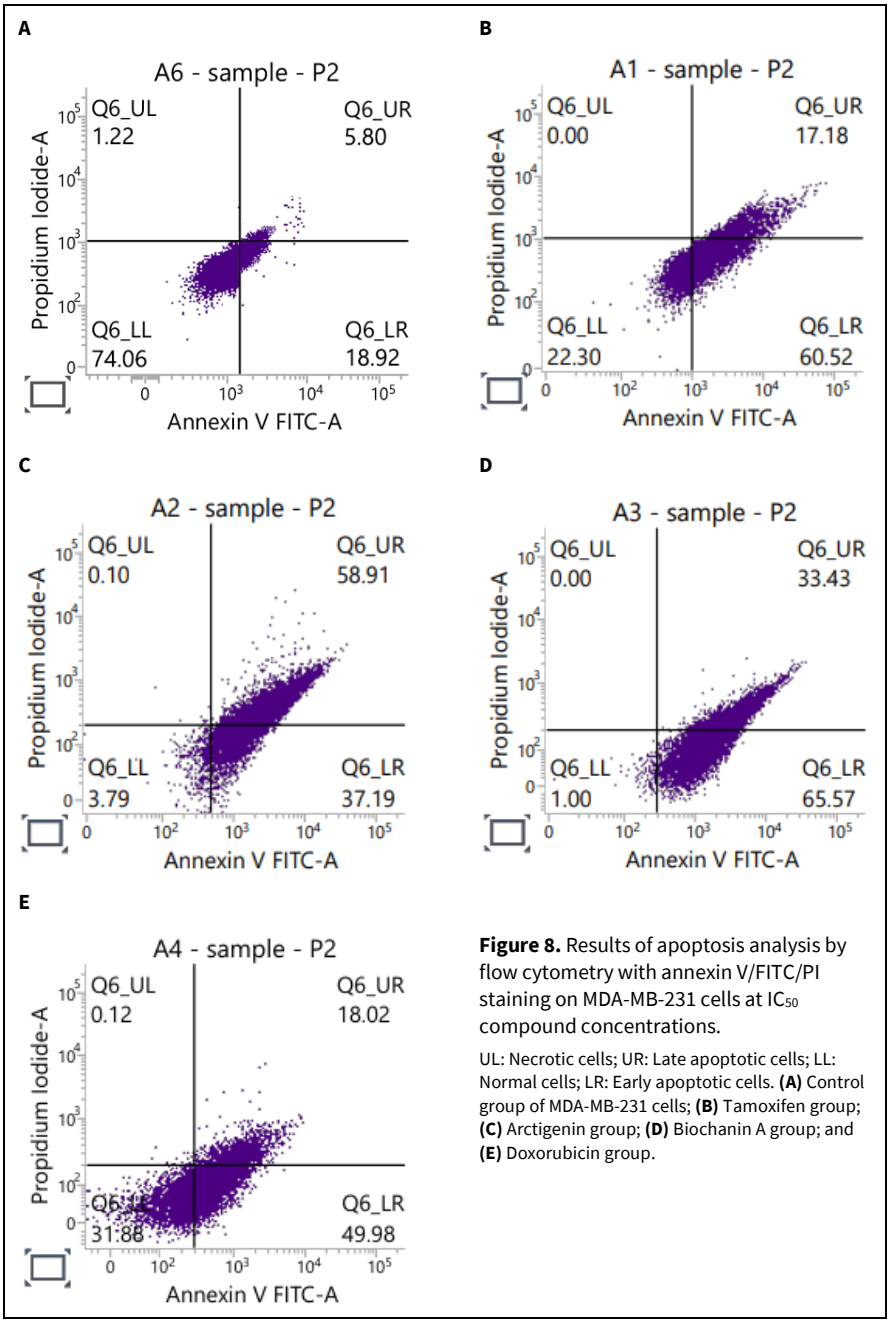

Figure 8. Results of apoptosis analysis by flow cytometry with annexin V/FITC/PI staining on MDA-MB-231 cells at IC_{50} compound concentrations.

UL: Necrotic cells; UR: Late apoptotic cells; LL: Normal cells; LR: Early apoptotic cells. **(A)** Control group of MDA-MB-231 cells; **(B)** Tamoxifen group; **(C)** Arctigenin group; **(D)** Biochanin A group; and **(E)** Doxorubicin group.

breast cancer progression, therapeutic resistance, and tumor heterogeneity (Xu et al., 2020). The pathway is also involved in the proliferation and survival of breast cancer cells, making it a potential target for the development of breast cancer therapies. Its activity centers on the key role of β-catenin (Wen et al., 2020). β-catenin is a central component of the canonical Wnt signaling pathway and a potential therapeutic target for breast cancer treatment. Inhibition of β-catenin has been shown to reduce breast cancer cell proliferation and induce apoptosis (Liu et al., 2022; Zhang and Wang, 2020). In this study, β-catenin was selected as the target protein, and its structure was used as a pharmacophore model for virtual screening.

In this study, pharmacophore analysis, binding energy, and inhibition constants were used to evaluate potential drug candidates. The pharmacophore fitness score, which measures the chemical and geometric features of a compound relative to a pharmacophore model, indicated that arctigenin and biochanin A had the best fitness. Binding energy, which measures the strength of interaction between a drug molecule and its target, showed that arctigenin and biochanin A had the lowest binding energies, indicating strong interactions. The inhibition constants (Ki), which reflect the binding affinity of a compound with its target, demonstrated that arctigenin and biochanin A had the lowest inhibition concentrations, indicating

high affinity as shown in Tables 2 and 4. Therefore, these results support arctigenin and biochanin A as potential drug candidates with good interactions with the target.

The positive controls used on MDA-MB-231 breast cancer cells were doxorubicin, tamoxifen, and cisplatin. MDA-MB-231 does not express estrogen receptor alpha (ERα) but has approximately 20-30% expression of estrogen receptor beta (ERβ). Although tamoxifen is commonly used to target ERα, research by Gruvberger-Saal et al. (2007) suggests the potential interaction of tamoxifen with the ERβ receptor in MDA-MB-231. Tamoxifen can affect ERβ and enhance nuclear respiratory factor 1 transcription (Gruvberger-Saal et al., 2007). The use of doxorubicin in this study is based on its role in TNBC therapy. Tamoxifen was used in this study due to its structural similarity to arctigenin and biochanin A.

This study evaluated the cytotoxic effects of arctigenin and biochanin A on triple-negative breast cancer cells MDA-MB-231 using MTT assays. Both compounds showed cytotoxic activity, with IC50 values of 42.903 µM and 244.386 µM, respectively, compared to the positive control tamoxifen (IC_{50} = 60.246 µM). These results are consistent with a study by Lou et al. (2017), where arctigenin affected the viability of MDA-MB-231 cells at a concentration of 40 µM. However, there are differences with the studies by Ren et al. (2018) and Darakhshan et al. (2015), possibly due to variations in experimental parameters such as the number of seeded cells, MTT concentration, incubation time, and type of culture media. In Ren et al. (2018) study, biochanin A was used at a concentration of 70 µM on MDA-MB-231 cells, with cells seeded at 5 × 10^4, while in this study, cells were seeded at 1 × 10^4. One of the differences between Darakhshan et al. (2015) study and this study is the serial concentrations used; the highest concentration of tamoxifen in Darakhshan's study was 20 µM, while in this study, it was 100 µM (Darakhshan et al., 2015; Ren et al., 2018). Pipetting factors may also contribute to the differences between these studies.

The test compounds, arctigenin and biochanin A, showed an increased risk of apoptosis-induced death in triple-negative breast cancer MDA-MB-231 cells. Both compounds induced total cell death through apoptosis at specific concentrations, indicating their potential as apoptosis agents. Annexin V and propidium iodide (PI) staining in apoptosis analysis allowed for the distinction between early apoptosis (annexin V positive, PI negative) and late apoptosis (annexin V positive, PI positive), enabling the detection of apoptosis stages. Arctigenin is known to induce apoptosis in triple-negative breast cancer (TNBC). A study showed that arctigenin causes significant cytotoxicity in TNBC cells, demonstrating its potential as a treatment for this type of cancer. Arctigenin has been proven to trigger apoptosis in breast cancer cells that do not express estrogen receptors through the ROS/p38 MAPK pathway (Feng et al., 2017). Additionally, arctigenin activates caspase-3 and poly (ADP-ribose) polymerase (PARP), leading to cell death. These findings support the potential of arctigenin as a compound that can induce apoptosis in TNBC cells (Shabgah et al., 2021).

Meanwhile, knowledge regarding the specific effects of biochanin A in inducing apoptosis in TNBC cells remains limited. Although biochanin A has shown apoptotic effects in other types of cancer cells, such as lung cancer and HER2-positive breast cancer cells, its impact on apoptosis in TNBC cells has not been widely documented in the available literature. Biochanin A inhibits the activity of MMP-2 and MMP-9 in HER2-positive breast cancer cells (Sehdev et al., 2009). Biochanin A is also known to reduce the expression of intrinsic anti-apoptotic factors like Bcl-2 and Bcl-xL, while increasing the levels and activation of intrinsic apoptotic factors such as Bad and caspase-9. Additionally, biochanin A induces the activation of caspase-3 and poly (ADP-ribose) polymerase (PARP) in FaDu cells (Cho et al., 2017). These findings support the potential of arctigenin and biochanin A as apoptosis agents in TNBC, with arctigenin showing more extensively documented mechanisms of action.

CONCLUSION

Arctigenin and biochanin A are phytoestrogen compounds that passed virtual screening and molecular simulations for TNBC drug discovery. Both compounds show potential anticancer effects on the MDA-MB-231 cell line. However, further research, including *in vivo* models, is needed to confirm arctigenin and biochanin A as the best candidates from virtual screening and molecular simulation.

CONFLICT OF INTEREST

The authors declare no conflicts of interest.

ACKNOWLEDGMENTS

The authors thank the PUTI Q2 2023 Universitas Indonesia grant for this manuscript.

REFERENCES

Alaouna M, Penny C, Hull R, Molefi T, Chauke-Malinga N, Khanyile R, Makgoka M, Bida M, Dlamini Z (2023) Overcoming the challenges of phytochemicals in triple negative breast cancer therapy: The path forward. Plants 12(12): 2350. https://doi.org/10.3390/plants12122350

Anandhi Senthilkumar H, Fata JE, Kennelly EJ (2018) Phytoestrogens: The current state of research emphasizing

breast pathophysiology. Phytother Res 32(9): 1707–1719. https://doi.org/10.1002/ptr.6115

Barrett T, Wilhite SE, Ledoux P, Evangelista C, Kim IF, Tomashevsky M, Marshall KA, Phillippy KH, Sherman PM, Holko M, Yefanov A, Lee H, Zhang N, Robertson CL, Serova N, Davis S, Soboleva A (2013) NCBI GEO: Archive for functional genomics data sets--update. Nucleic Acids Res 41(Database issue): D991–D995. https://doi.org/10.1093/nar/gks1193

Batool M, Ahmad B, Choi S (2019) A structure-based drug discovery paradigm. Int J Mol Sci 20(11): 2783. https://doi.org/10.3390/ijms20112783

Chen T, Shu X, Zhou H, Beckford FA, Misir M (2023) Algorithm selection for protein-ligand docking: Strategies and analysis on ACE. Sci Rep 13(1): 8219. https://doi.org/10.1038/s41598-023-35132-5

Cho IA, You SJ, Kang KR, Kim SG, Oh JS, You JS, Lee GJ, Seo YS, Kim DK, Kim CS, Lee SY, Kim JS (2017) Biochanin-A induces apoptosis and suppresses migration in FaDu human pharynx squamous carcinoma cells. Oncol Rep 38(5): 2985–2992. https://doi.org/10.3892/or.2017.5953

Collignon J, Lousberg L, Schroeder H, Jerusalem G (2016) Triple-negative breast cancer: treatment challenges and solutions. Breast Cancer 8: 93–107. https://doi.org/10.2147/bctt.s69488

Darakhshan S, Ghanbari A, Gholami Rad F, Bidmeshki Pour A (2015) Tamoxifen and tranilast show a synergistic effect against breast cancer *in vitro*. Bratisl Lek Listy 116(1): 69–73. https://doi.org/10.4149/bll_2015_013

Fadilah F, Kezia I, Erlina L (2024) Uncovering potential neuroprotective flavonoids for Alzheimer's disease using cutting-edge molecular simulation and *in vitro* SHSY-5Y analysis. J Pharm Pharmacogn Res 12(2): 204–217. https://doi.org/10.56499/jppres23.1715_12.2.204

Feng T, Cao W, Shen W, Zhang L, Gu X, Guo Y, Tsai HI, Liu X, Li J, Zhang J, Li S, Wu F, Liu Y (2017) Arctigenin inhibits STAT3 and exhibits anticancer potential in human triple-negative breast cancer therapy. Oncotarget 8(1): 329–344. https://doi.org/10.18632/oncotarget.13393

Ferreira LG, Dos Santos RN, Oliva G, Andricopulo AD (2015) Molecular docking and structure-based drug design strategies. Molecules 20(7): 13384–13421. https://doi.org/10.3390/molecules200713384

Freelander A, Brown LJ, Parker A, Segara D, Portman N, Lau B, Lim E (2021) Molecular biomarkers for contemporary therapies in hormone receptor-positive breast cancer. Genes 12(2): 285. https://doi.org/10.3390/genes12020285

Gruvberger-Saal SK, Bendahl PO, Saal LH, Laakso M, Hegardt C, Edén P, Peterson C, Malmström P, Isola J, Borg A, Fernö M (2007) Estrogen receptor beta expression is associated with tamoxifen response in ERalpha-negative breast carcinoma. Clin Cancer Res 13(7):1987–1994. https://doi.org/10.1158/1078-0432.ccr-06-1823

Ko KP, Yeo Y, Yoon JH, Kim CS, Tokudome S, Ngoan LT, Koriyama C, Lim YK, Chang SH, Shin HR, Kang D, Park SK, Kang CH, Yoo KY (2018) Plasma phytoestrogens concentration and risk of colorectal cancer in two different Asian populations. Clin Nutr 37(5): 1675–1682. https://doi.org/10.1016/j.clnu.2017.07.014

Lionta E, Spyrou G, Vassilatis DK, Cournia Z (2014) Structure-based virtual screening for drug discovery: Principles, applications and recent advances. Curr Top Med Chem 14(16):1923–1938. https://doi.org/10.2174/1568026614666140929124445

Liu J, Xiao Q, Xiao J, Niu C, Li Y, Zhang X, Zhou Z, Shu G, Yin G (2022) Wnt/β-catenin signalling: function, biological mechanisms, and therapeutic opportunities. Signal Transduct Target Ther 7(1): 3. https://doi.org/10.1038/s41392-021-00762-6

Lou C, Zhu Z, Zhao Y, Zhu R, Zhao H (2017) Arctigenin, a lignan from *Arctium lappa* L., inhibits metastasis of human breast cancer cells through the downregulation of MMP-2/-9 and heparanase in MDA-MB-231 cells. Oncol Rep 37(1): 179–184. https://doi.org/10.3892/or.2016.5269

Mabonga L, Kappo AP (2019) Protein-protein interaction modulators: Advances, successes and remaining challenges. Biophys Rev 11(4): 559–581. https://doi.org/10.1007/s12551-019-00570-x

Makki J (2015) Diversity of breast carcinoma: Histological subtypes and clinical relevance. Clin Med Insights Pathol 8: 23–31. https://doi.org/10.4137/cpath.s31563

Moore TJ, Zhang H, Anderson G, Alexander GC (2018) Estimated costs of pivotal trials for novel therapeutic agents approved by the US Food and Drug Administration, 2015-2016. JAMA Intern Med 178(11): 1451–1457. https://doi.org/10.1001/jamainternmed.2018.3931

Orrantia-Borunda E, Anchondo-Nuñez P, Acuña-Aguilar LE, Gómez-Valles FO, Ramírez-Valdespino CA (2022) Subtypes of Breast Cancer. In: Mayrovitz HN, editor. Breast Cancer [Internet]. Brisbane (AU): Exon Publications; Aug 6. Chapter 3. https://doi.org/10.36255/exon-publications-breast-cancer-subtypes

Park J, Son A, Kim H (2023) A protein-protein interaction analysis tool for targeted cross-linking mass spectrometry. Sci Rep 13(1): 22103. https://doi.org/10.1038/s41598-023-49663-4

Pedretti A, Mazzolari A, Gervasoni S, Vistoli G (2019) Rescoring and linearly combining: A highly effective consensus strategy for virtual screening campaigns. Int J Mol Sci 20(9): 2060. https://doi.org/10.3390/ijms20092060

Ren G, Shi Z, Teng C, Yao Y (2018) Antiproliferative activity of combined biochanin A and ginsenoside Rh_2 on MDA-MB-231 and MCF-7 human breast cancer cells. Molecules 23(11): 2908. https://doi.org/10.3390/molecules23112908

Sehdev V, Lai JC, Bhushan A (2009) Biochanin A modulates cell viability, invasion, and growth promoting signaling pathways in HER-2-positive breast cancer cells. J Oncol 2009:121458. https://doi.org/10.1155/2009/121458

Shaath H, Elango R, Alajez NM (2021) Molecular classification of breast cancer utilizing long non-coding RNA (lncRNA) transcriptomes identifies novel diagnostic lncRNA panel for triple-negative breast cancer. Cancers 13(21): 5350. https://doi.org/10.3390/cancers13215350

Shabgah AG, Suksatan W, Achmad MH, Bokov DO, Abdelbasset WK, Ezzatifar F, Hemmati S, Mohammadi H, Soleimani D, Jadidi-Niaragh F, Ahmadi M, Navashenaq JG (2021) Arctigenin, an anti-tumor agent; a cutting-edge topic and up-to-the-minute approach in cancer treatment. Eur J Pharmacol 909: 174419. https://doi.org/10.1016/j.ejphar.2021.174419

Sung H, Ferlay J, Siegel RL, Laversanne M, Soerjomataram I, Jemal A, Bray F (2021) Global Cancer Statistics 2020: GLOBOCAN estimates of incidence and mortality worldwide for 36 cancers in 185 countries. CA Cancer J Clin 71(3): 209–249. https://doi.org/10.3322/caac.21660

Telford WG (2018) Multiparametric Analysis of Apoptosis by Flow Cytometry. Methods Mol Biol 1678: 167–202. https://doi.org/10.1007/978-1-4939-7346-0_10

Torrens-Mas M, Roca P (2020) Phytoestrogens for cancer prevention and treatment. Biology 9(12): 427. https://doi.org/10.3390/biology9120427

van Barele M, Heemskerk-Gerritsen BAM, Louwers YV, Vastbinder MB, Martens JWM, Hooning MJ, Jager A (2021) Estrogens and progestogens in triple negative breast cancer: Do they harm?

Cancers 13(11): 2506. https://doi.org/10.3390/cancers13112506

Wen X, Wu Y, Awadasseid A, Tanaka Y, Zhang W (2020) New advances in canonical Wnt/β-catenin signaling in cancer. Cancer Manag Res 12: 6987–6998. https://doi.org/10.2147/cmar.s258645

Xiong N, Wu H, Yu Z (2024) Advancements and challenges in triple-negative breast cancer: A comprehensive review of therapeutic and diagnostic strategies. Front Oncol 14: 1405491. https://doi.org/10.3389/fonc.2024.1405491

Xu X, Zhang M, Xu F, Jiang S (2020) Wnt signaling in breast cancer: Biological mechanisms, challenges and opportunities. Mol Cancer 9(1): 165. https://doi.org/10.1186/s12943-020-01276-5

Yang L, Wu X, Wang Y, Zhang K, Wu J, Yuan YC, Deng X, Chen L, Kim CC, Lau S, Somlo G, Yen Y (2011) FZD7 has a critical role in cell proliferation in triple negative breast cancer. Oncogene 30(43): 4437–4446. https://doi.org/10.1038/onc.2011.145

Yin L, Duan JJ, Bian XW, Yu SC (2020) Triple-negative breast cancer molecular subtyping and treatment progress. Breast Cancer Res 22(1): 61. https://doi.org/10.1186/s13058-020-01296-5

Zhang Y, Wang X (2020) Targeting the Wnt/β-catenin signaling pathway in cancer. J Hematol Oncol 13(1): 165. https://doi.org/10.1186/s13045-020-00990-3

AUTHOR CONTRIBUTION:

Contribution	Arsianti A	Akbar MK	Erlina L
Concepts or ideas	x	x	x
Design	x		x
Definition of intellectual content	x		x
Literature search		x	
Experimental studies		x	
Data acquisition		x	
Data analysis	x	x	
Statistical analysis	x	x	
Manuscript preparation		x	x
Manuscript editing	x	x	x
Manuscript review	x	x	x

Citation Format: Arsianti A, Akbar MK, Erlina L (2025) Arctigenin and biochanin A impact on MDA-MB-231 breast cancer cells: *In silico* and *in vitro* analysis. J Pharm Pharmacogn Res 13(2): 606–620. https://doi.org/10.56499/jppres24.2024_13.2.606

Publisher's Note: All claims expressed in this article are solely those of the authors and do not necessarily represent those of their affiliated organizations, or those of the publisher, the editors and the reviewers. Any product that may be evaluated in this article, or claim that may be made by its manufacturer, is not guaranteed or endorsed by the publisher.

Open Access: This article is distributed under the terms of the Creative Commons Attribution 4.0 International License (http://creativecommons.org/ licenses/by/4.0/), which permits use, duplication, adaptation, distribution and reproduction in any medium or format, as long as you give appropriate credit to the original author(s) and the source, provide a link to the Creative Commons license and indicate if changes were made.